THE JOURNAL OF PHYSICAL CHEMISTRY A
A JOURNAL OF THE AMERICAN CHEMICAL SOCIETY

pubs.acs.org/JPCA Article

Probing the Location of Hydrogen Atoms in Low-Barrier Hydrogen Bonds in 1,3-Diketone Molecules by H/D Isotope Shifts in Solid-State ^{17}O Nuclear Magnetic Resonance and ^{1}H−^{17}O Distance Measurements

Gang Wu,* Yizhe Dai, Ivan Hung, Zhehong Gan, Maria A. Matlinska, and Roderick E. Wasylishen

Cite This: *J. Phys. Chem. A* 2025, 129, 5993−6003 Read Online

ACCESS | Metrics & More | Article Recommendations | Supporting Information

ABSTRACT: 1,3-Diketone molecules existing in their *cis*-keto−enol tautomeric forms in the solid state are classic examples that contain low-barrier hydrogen bonds (LBHBs) of the O−H···O type. We report experimental observations of H/D isotope shifts in ^{13}C and ^{17}O solid-state nuclear magnetic resonance (NMR) spectra of three representative 1,3-diketone molecules: dibenzoylmethane, benzoylacetone, and curcumin. While there are several examples of H/D isotope shifts in solid-state ^{13}C NMR spectra in the literature, this study reports on the first observation of such H/D isotope shifts in solid-state ^{17}O NMR spectra. We found that the H/D isotope shifts in dibenzoylmethane are considerably larger than those in benzoylacetone and curcumin. To aid interpretation of the observed H/D isotope shifts, we performed direct ^{1}H−^{17}O distance measurement using two-dimensional ^{17}O/^{1}H quadrupole−dipole correlation NMR spectroscopy. The results of ^{1}H−^{17}O distance measurements provided direct evidence about the "location" of the enol hydrogen atom in the ^{17}O···^{1}H···^{17}O LBHBs. We demonstrated that H/D isotope shifts in solid-state ^{17}O NMR and ^{1}H−^{17}O distance measurement are two new ways of probing the nature of LBHBs. Our new solid-state ^{17}O NMR results are discussed in connection to nuclear quantum effects (i.e., the potential energy curve, zero-point energy, and nuclear wave function) and high-quality structural data available for these compounds in the literature.

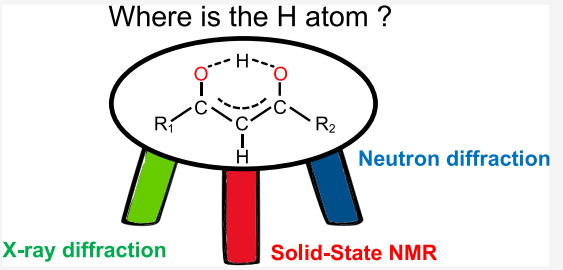

1. INTRODUCTION

Nuclear quantum effects such as zero-point motion, nuclear wave function, and tunneling are known to be important in many chemical and biological processes.[1−9] Among the various related topics, the quantum nature of hydrogen bonds is a particularly intriguing one due to the fundamental importance of hydrogen bonds in both the structures and functions of biological systems.[10−21] Because the proton is the lightest atomic nucleus, significant nuclear quantum effects are generally expected in many X−H···Y hydrogen bonds where X and Y are donor and acceptor atoms, respectively. This is particularly true in the cases of short hydrogen bonds. For short hydrogen bonds where the separations between X and Y atoms are as short as ca. 2.4−2.6 Å, the potential energy surface for proton migration across the hydrogen bond typically either is a rather flat single well or exhibits a small barrier between two energy minima. The latter cases are often known as low-barrier hydrogen bonds (LBHBs).[22−27]

In this study, we focus on LBHBs in the solid state. In the literature, considerable attention has been devoted either to determine the "location" of the hydrogen atom in LBHBs or to examine the hydrogen atom "migration" in LBHBs as a function of temperature or pressure. We recognize that it is still customary, especially among crystallographers, to identify a single point (e.g., the highest point in the nuclear density map from neutron diffraction data) as the "location" of the hydrogen atom. However, in the context of nuclear quantum effects, a proton should be viewed in terms of its nuclear wave function. In this work, when we use the term "location of the hydrogen atom", we generally refer to the three-dimensional shape of the nuclear wave function of the proton in question rather than just a single point in space. This is particularly important when dealing with LBHBs where the proton is indeed delocalized. Of course, the problem is that no currently available technique is capable of revealing a detailed 3D nuclear wave function. Nonetheless, several experimental techniques have been employed to obtain information about the "location" of the hydrogen atom in LBHBs. Single-crystal neutron and X-ray diffraction methods are no doubt the most

Received: April 8, 2025
Revised: June 4, 2025
Accepted: June 13, 2025
Published: June 26, 2025

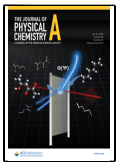

https://doi.org/10.1021/acs.jpca.5c02392
J. Phys. Chem. A 2025, 129, 5993−6003

reliable techniques that can produce the most direct structural information. It is also known that the two diffraction techniques may produce slightly different pictures about the "location" of the hydrogen atom in LBHBs.[28] Neutron diffraction is expected to yield the most reliable information as this technique measures the nuclear density directly. In neutron diffraction studies, it is a common practice to report the highest nuclear density point as the "location" of the hydrogen atom together with atomic displacement ellipsoids. In LBHBs, the "spread" of the nuclear density distribution (i.e., zero-point motion) is critically important. Unfortunately, neutron diffraction experiments are currently unable to produce an accurate three-dimensional "shape" for the proton density distribution. Solid-state NMR is another powerful technique that can offer structural, spectroscopic, and dynamic parameters that may be linked to the "location" of the hydrogen atom in LBHBs.[29−33] In addition to experimental techniques, state-of-the-art computational approaches such as *ab initio* path-integral molecular dynamics (PIMD) simulations have begun to be able to accurately treat nuclear quantum effects.[34−37]

In this study, we used two solid-state NMR techniques to probe the "location" of hydrogen atoms in LBHBs present in three representative 1,3-diketone compounds: dibenzoylmethane, benzoylacetone, and curcumin; see Scheme 1.

Scheme 1. Resonance Structures in 1,3-Diketone Compounds and Molecular Structures of Dibenzoylmethane, Benzoylacetone, and Curcumin

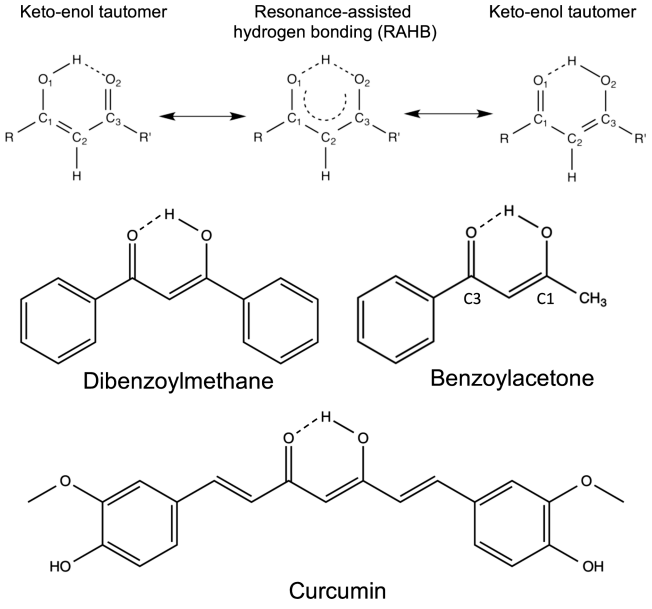

Traditionally, chemists think of these 1,3-diketone molecules in terms of their different tautomers resulting in a resonance-assisted hydrogen bond, as shown in Scheme 1. Now, it is widely recognized that the hydrogen bonding in these compounds can be better viewed in terms of nuclear wave functions and that these compounds very often form LBHBs. First, we attempted to simultaneously measure the H/D isotope shifts in ^{13}C and ^{17}O solid-state NMR spectra when the enol hydrogen (H) is replaced by deuterium (D). While H/D isotope shifts are known to be sensitive to hydrogen bonding,[38−41] this phenomenon has rarely been examined in solid-state NMR studies of LBHBs. We should note, however, that H/D isotope shifts have indeed been reported in previous solution NMR studies of 1,3-diketone compounds.[42−49] Second, we used a solid-state NMR technique known as two-dimensional (2D) $^{17}O/^{1}H$ quadrupole-dipole (QD) correlation spectroscopy[50] to directly measure the $^{1}H-^{17}O$ distance between the enol hydrogen atom and the two surrounding oxygen atoms. Since the two oxygen nuclei of the O−H···O fragment generally have different ^{17}O chemical shifts,[51,52] we demonstrate that the O−H and H···O distances can be measured simultaneously. This would yield direct information about the "location" of the enol hydrogen atom. Again, while $^{1}H-^{17}O$ distance measurement has been previously demonstrated in both inorganic and organic solids,[53−57] its application to LBHBs in 1,3-diketone compounds has not been explored to the best of our knowledge. It should, however, be noted that $^{1}H-^{15}N$ distance measurement by solid-state NMR has been reported in the literature for several N−H···N LBHBs.[58,59] The reason why we chose the three 1,3-diketone compounds shown in Scheme 1 was that these compounds are classic examples of LBHBs that have been extensively studied by neutron and X-ray diffraction,[28,60−71] solid-state ^{1}H, ^{2}H, ^{13}C, and ^{17}O NMR,[72−79] *ab initio* quantum chemical calculations,[32,68,80−82] and PIMD simulations.[83,84]

Dibenzoylmethane crystallizes in three crystal polymorphs: a stable orthorhombic form, space group P_{bca}, $Z = 8$;[60,61,63] a metastable orthorhombic form;[85] and a monoclinic form, space group $P2_1/c$, $Z = 4$.[63,86] The stable orthorhombic polymorph is the most common one and was simultaneously studied by X-ray and neutron diffraction over the temperature range between 100 and 280 K.[28] There is no evidence of any phase transition in this temperature range. Solid-state ^{1}H, ^{13}C, and ^{17}O NMR data for this stable orthorhombic polymorph of dibenzoylmethane are available in the literature.[32,75] Benzoylacetone is known to crystallize only in the monoclinic crystal form, space group $P2_1/c$, $Z = 4$.[62,64−66] This polymorph was later extensively studied by X-ray and neutron diffraction between 8 and 300 K.[67] Again, no phase transition was observed for benzoylacetone over this large temperature range. In addition, high-quality crystal structures for the deuterated form of benzoylacetone were also obtained from X-ray and neutron diffraction data collected at 11−15 K.[68] Curcumin is known to exist in three polymorphs: form I, monoclinic space group $P2_1/n$, $Z = 4$, $Z' = 1$; form II, orthorhombic space group $Pca2_1$, $Z = 8$, $Z' = 2$; and form III, orthorhombic space group $Pbca$, $Z = 8$, $Z' = 1$.[71] Form I is the most stable polymorph of curcumin.[87] Solid-state ^{1}H, ^{13}C, and ^{17}O NMR data have been reported for all three crystal forms in the literature.[32,71,77,79]

The primary goal of the present study is to investigate whether the two new solid-state NMR techniques can provide additional insight into the nature of LBHBs in these model systems. For each compound, we chose to study the most stable and well-characterized polymorph. This study was also part of our continuing effort to apply solid-state ^{17}O NMR spectroscopy in studies of hydrogen-bonded systems.[88−94]

2. EXPERIMENTAL SECTION

Preparations of [1,3-$^{17}O_2$]-dibenzoylmethane, [1,3-$^{17}O_2$]-curcumin, [1,2-$^{17}O_2$]-salicylic acid (2-hydroxybenzoic acid), and [3-^{17}O]-salicylic acid were reported previously.[32,79,95] [1,3-$^{17}O_2$]-Benzoylacetone was synthesized with the same procedure as for [1,3-$^{17}O_2$]-dibenzoylmethane. The ^{17}O enrichment level was about 20% in all compounds.

https://doi.org/10.1021/acs.jpca.5c02392
J. Phys. Chem. A 2025, 129, 5993−6003

Deuteration of each of the three 1,3-diketone compounds was achieved by repeated recrystallization from methanol-d_1. The final level of deuteration in each compound was estimated to be greater than 90% by comparing ^{1}H magic-angle-spinning (MAS) NMR spectra between the H and D forms of the compound. To confirm that the correct polymorph of the solid compound was prepared in each case, powder X-ray diffractions patterns were recorded and compared with the theoretical patterns; see Figure S1 in the Supporting Information. In this regard, solid-state ^{1}H, ^{13}C, and ^{17}O NMR spectra were also used in some cases to help identify the polymorph of the compound because the NMR parameters were linked to different polymorphs on the basis of plane-wave DFT calculations.[32,71,77,79]

Solid-state ^{1}H, ^{17}O, and ^{13}C NMR experiments were performed on a Bruker NEO-700 NMR spectrometer (16.4 T) with a 2.5 mm HXY MAS probe at Queen's University. In the ^{13}C 20 kHz cross-polarization (CP) MAS experiments, a contact time of 2 ms was used and the ^{1}H decoupling field was about 100 kHz. A rotor-synchronized Hahn-echo sequence was used for recording both ^{1}H and ^{17}O 30 kHz MAS NMR spectra to eliminate the acoustic ringing and the background signal from the probe. For the ^{17}O MAS experiments, no proton decoupling was applied during data acquisition. The 90° pulse width for the ^{17}O central transition was 1.0 μs. The recycle delays used in different solid-state NMR experiments were 60 s for ^{1}H, 10 s for ^{13}C, and 5 s for ^{17}O. Sample temperatures under MAS conditions with the 2.5 mm HXY probe were calibrated with the ^{79}Br NMR signal from a solid KBr sample.[96] Typically, the BCU II was set to 273 K, so that the true sample temperature with frictional heating was at 285 (with 20 kHz MAS) and 308 K (with 30 kHz MAS). All ^{13}C chemical shifts were referenced to the signal of 1% TMS in $CDCl_3$ (δ = 0 ppm) by setting the ^{13}C NMR signal of the C=O group of solid α-glycine to 176.5 ppm.[97] Once the ^{13}C chemical shift referencing was set, ^{1}H and ^{17}O chemical shift references, 1% TMS in $CDCl_3$ and neat H_2O(liq), respectively, were calculated by using the frequency ratio (Ξ) values from the literature (for ^{1}H, Ξ = 100.000000%; for ^{13}C, Ξ = 25.145020%; for ^{17}O, Ξ = 13.556457%).[98] In our experience, this systematic way of simultaneous setting the ^{1}H, ^{13}C, and ^{17}O references can reliably produce an accuracy of chemical shifts within 0.1 ppm.

The 2D ^{17}O/^{1}H quadrupole−dipole (QD) correlation spectra[50] were acquired at the National High Magnetic Field Laboratory (NHMFL, Tallahassee, Florida, USA) using the 21.1 T ultrawide bore magnet equipped with a Bruker AVANCE III console and a 3.2 mm HX transmission line probe designed and built at the NHMFL. Experiments were performed at the Larmor frequencies of 899.1 and 121.9 MHz for ^{1}H and ^{17}O, respectively. The sample spinning frequency was 17 kHz. Selective ^{17}O $\pi/2$ and π pulses for the central transition were 2.0 and 4.0 μs, respectively, which corresponds to a $B_1(^{17}O)$ field of 41.7 kHz. Dipolar recoupling was applied to the ^{1}H nuclei using the $R18^5_2$ symmetry-based sequence, which requires an RF field of 4.5 times the sample spinning frequency. A t_1 increment of 117.6 μs in the ^{1}H−^{17}O dipolar recoupling period was used in all 2D QD experiments. Other acquisition parameters are as follows: [1,3-$^{17}O_2$]-dibenzoylmethane, 30 t_1 increments, 256 transients per t_1, and 0.5 s recycle delay; [1,3-$^{17}O_2$]-benzoylacetone, 30 t_1 increments, 256 transients per t_1, and 0.2 s recycle delay; [1,3-$^{17}O_2$]-curcumin, 20 t_1 increments, 3072 transients per t_1, and 0.5 s recycle delay. Numerical simulations to extract ^{1}H−^{17}O dipolar couplings from 2D QD spectra were performed with SIMPSON.[99] A sample input file is provided in the Supporting Information.

3. RESULTS AND DISCUSSION

Figure 1 shows the ^{1}H, ^{13}C, and ^{17}O MAS NMR spectra recorded for both protonated and deuterated versions of the three 1,3-diketone compounds. All solid-state NMR parameters extracted from these spectra are summarized in Table 1. The ^{1}H chemical shifts observed for the enol hydrogen atoms in dibenzoylmethane, benzoylacetone, and curcumin are 17.5 ± 0.1, 16.2 ± 0.1, and 16.9 ± 0.1 ppm, respectively. These values are consistent with the previously reported solid-state ^{1}H NMR data for these compounds.[32,75] In addition, the ^{1}H MAS spectra provide a means of measuring the deuteration level for the enol hydrogen. We found that the degree of deuteration in all three compounds was greater than 90%. Figure 1 also displays the C1 and C3 signals from the ^{13}C CP/MAS spectra obtained for the protonated and deuterated compounds; full ^{13}C CP/MAS spectra for the six compounds are provided in the Supporting Information. Clearly, replacing the enol H with D causes small changes in the ^{13}C chemical shifts for the C1 and C3 atoms, reflecting the H/D isotope effect. In this study, we followed Hansen and co-workers[40,44−47,49,100] to use the following definition for the H/D isotope shifts on the X nucleus:

$$^n\Delta X(H/D) = \delta X(H) - \delta X(D) \quad (1)$$

where n is the number of chemical bonds that separate the observed nucleus X and H/D. We should note that another

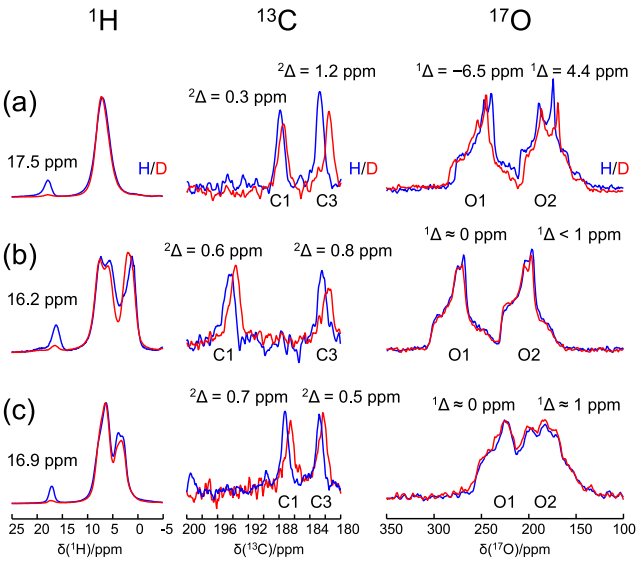

Figure 1. Comparison of ^{1}H, ^{13}C, and ^{17}O MAS NMR spectra obtained for protonated (H, blue traces) and deuterated (D, red traces) forms of (a) [1,3-$^{17}O_2$]-dibenzoylmethane, (b) [1,3-$^{17}O_2$]-benzoylacetone, and (c) [1,3-$^{17}O_2$]-curcumin. All spectra were recorded at 16.4 T. The sample spinning frequency was 30 kHz in the ^{1}H and ^{17}O MAS experiments (the true sample temperature was 308 K) and 20 kHz in the ^{13}C NMR experiments (the true sample temperature was 285 K). Note that, in each case, only the ^{13}C NMR signals from the *cis*-keto−enol moiety are shown. The entire ^{13}C CP/MAS spectra for the six compounds can be found in the Supporting Information. For clarity, the simulated ^{17}O MAS spectra are not shown here, and they are provided in the Supporting Information.

https://doi.org/10.1021/acs.jpca.5c02392
J. Phys. Chem. A 2025, 129, 5993−6003

Table 1. Summary of Experimental ^{1}H, ^{13}C, and ^{17}O Solid-State NMR Parameters Obtained for Dibenzoylmethane, Benzoylacetone, and Curcumin in This Study[a]

		$\delta(^{13}C)$ (ppm)		$\delta(^{17}O)$ (ppm)		$C_Q(^{17}O)$ (MHz)		η_Q	
compd	$\delta(^{1}H)$ (ppm)	C1	C3	O1	O2	O1	O2	O1	O2
dibenzoylmethane-H	17.5	187.9	182.8	278.0	211.6	6.3	6.2	0.80	0.54
dibenzoylmethane-D		187.6	181.6	284.5	207.2	6.5	6.3	0.75	0.48
benzoylacetone-H	16.2	194.3	182.5	304.0	231.0	6.1	6.0	0.80	0.75
benzoylacetoneA-D		193.7	181.7	304.0	231.5	5.9	5.9	0.80	0.75
curcumin-H	16.9	187.3	182.8	256.0	208.0	6.0	6.4	0.85	0.60
curcumin-D		186.6	182.3	256.0	209.0	5.9	6.4	0.85	0.55

[a]The uncertainties in experimental values for $\delta(^{1}H)$, $\delta(^{13}C)$, $\delta(^{17}O)$, $C_Q(^{17}O)$, and η_Q are ±0.1, ±0.1 ppm, ±1.0 ppm, ±0.2 MHz, and ±0.05, respectively.

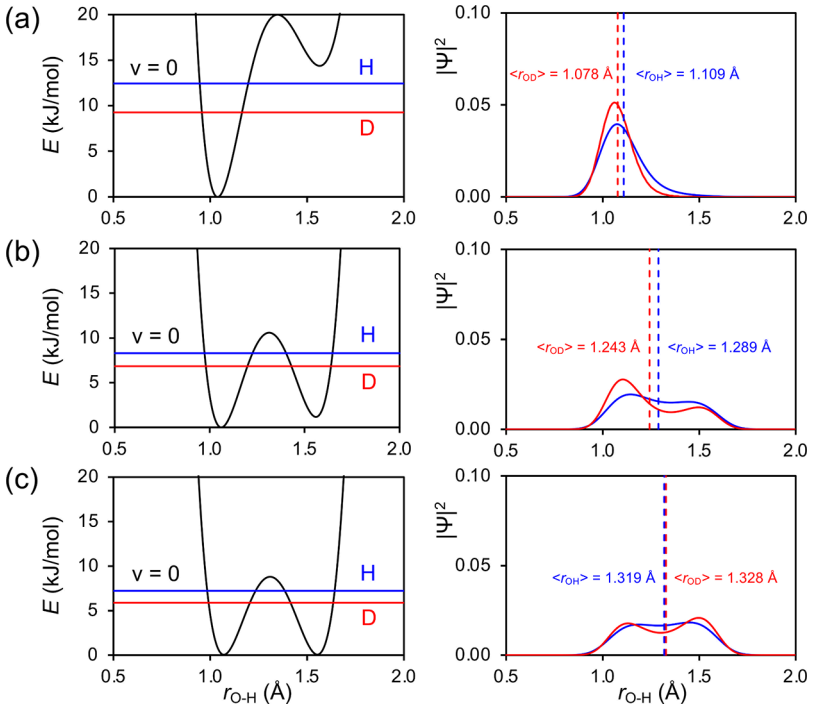

Figure 2. (a–c) Three 1D potential energy curves (left panel) and ground-state nuclear wave functions (right panel). Detailed parameters for the potential curves are given in the Supporting Information. The nuclear wave functions were obtained by solving the 1D Schrödinger equation with the Numerov method implemented in Excel.[103] The zero-point energies for H (blue line) and D (red line) are indicated.

definition for the isotope shift, introduced by Jameson,[101] would give the opposite sign. Because both definitions are commonly used in the literature, one should be careful when comparing isotope shift data from different studies.

As seen in Figure 1, all observed $^{2}\Delta^{13}C(H/D)$ values are positive. The largest value found in this study was that observed for the C3 atom of dibenzoylmethane, $^{2}\Delta^{13}C(H/D) = 1.2 \pm 0.2$ ppm. The C1 atom in dibenzoylmethane, however, displays the smallest H/D isotope shift, $^{2}\Delta^{13}C(H/D) = 0.3$ ppm. In the solid state, crystal packing effects cause the two halves of the dibenzoylmethane molecule to become non-equivalent, so that two ^{13}C NMR signals are observed for the *cis*-keto–enol moiety. This allows the detection of different $^{2}\Delta^{13}C(H/D)$ values for C1 and C3 nuclei. In solution, in contrast, only one ^{13}C NMR signal was observed for C1 and C3 nuclei at 185.65 ± 0.01 ppm with $^{2}\Delta^{13}C(H/D)$ being 0.63 ppm.[48] Interestingly, this $^{2}\Delta^{13}C(H/D)$ value is very close to the average of the two values observed in the solid state for dibenzoylmethane, i.e., $(1.2 + 0.3)/2 \approx 0.8$ ppm. For benzoylacetone and curcumin in the solid state, the C1 and C3 nuclei show similar H/D isotope shifts on the order of 0.5–0.8 ppm. Furthermore, the H/D isotope shifts do not appear to be correlated to the ^{13}C chemical shift difference between C1 and C3. This is because the actual ^{13}C chemical shifts for C1 and C3 are determined by the nature of the chemical groups on both sides of the *cis*-keto–enol moiety, whereas the H/D isotope shifts are sensitive solely to the hydrogen bonding within the *cis*-keto–enol moiety, i.e., C1═O1···(H/D)–O2–C3.

Now, let us examine the H/D isotope shifts on the ^{17}O nucleus in these compounds. As shown in Figure 1, we observed that upon deuteration of the enol hydrogen of dibenzoylmethane, the ^{17}O NMR signals for O1 and O2 are shifted to opposite directions. This is similar to what was reported in previous solution ^{17}O NMR studies of related compounds by Liepins et al.[48] and by Bolvig et al.[49] For dibenzoylmethane, we observed $^{1}\Delta^{17}O(H/D) = 4.4 \pm 1.0$ ppm for O2 and $^{1h}\Delta^{17}O(H/D) = -6.5 \pm 1.0$ ppm for O1. This is the first report of H/D isotope shifts in solid-state ^{17}O NMR. For benzoylacetone and curcumin, in contrast, all $^{1}\Delta^{17}O(H/$

https://doi.org/10.1021/acs.jpca.5c02392
J. Phys. Chem. A 2025, 129, 5993–6003

D) and $^{1h}\Delta^{17}O(H/D)$ values are too small to be reliably measured. Here, we introduce the $^{1h}\Delta^{17}O(H/D)$ notation (where the superscript 1h stands for "one hydrogen bond") to describe the H/D isotope shift for O1 in the *cis*-keto−enol geometry of the C1═O1···(H/D)−O2−C3 type. Note that previous studies[48,49] used the $^{5}\Delta^{17}O(H/D)$ notation. We believe that our notation better reflects the hydrogen bonding nature between the H and O atoms instead of emphasizing that there are five covalent bonds connecting the H and O atoms. Furthermore, the $^{1h}\Delta^{17}O(H/D)$ notation also closely resembles that used to describe the *J* coupling constant across a hydrogen bond, $^{1h}J(^{1}H, ^{17}O)$ or $^{1h}J(^{1}H, ^{15}N)$.[102] As seen in Figure 1, while the ^{17}O NMR signals suffer from second-order quadrupole broadening, it is still possible to measure H/D isotope shifts on the order of 1 ppm. Similar to the ^{13}C NMR results mentioned earlier, two ^{17}O NMR signals were observed for O1 and O2 nuclei for dibenzoylmethane due to crystal packing and they exhibit H/D isotope shifts with opposite signs. In solution, only one ^{17}O NMR signal was observed for O1 and O2 because of rapid exchange of the proton between the enol (C−OH) and keto (C═O) sites and the H/D isotope shift of −0.2 ppm was quite small.[48] This value can be compared with the average of the two solid-state values, i.e., $(-6.5 + 4.4)/2 \approx -1.0$ ppm. So far, the H/D isotope shift data on both ^{13}C and ^{17}O nuclei indicate that the LBHB in dibenzoylmethane appears to be quite different from those in benzoylacetone and curcumin.

To aid the interpretation of the observed H/D isotope shifts in these compounds, we consider three 1D O···H−O hydrogen bond models. Figure 2 shows the 1D potential energy curves for the three models. The first model, shown in Figure 2a, depicts a highly asymmetric double-well potential where the asymmetry is so large that the vibrational ground state lies well below the barrier for proton transfer. This kind of potential energy curve can be used to describe a regular (and weak) hydrogen bond. The second model in Figure 2b describes the situation of an LBHB where the two wells are slightly asymmetric. The third model is also an LBHB but with two nearly symmetric wells. Figure 2 also shows the numerically solved nuclear wave functions for H and D in the vibrational ground state for each of the three potential curves.

It has been well-established that the origin of H/D isotope shifts arises from the fact that the vibrationally averaged X−D bond is slightly shorter than the corresponding X−H bond.[104,105] As illustrated in Figure 2a, the r_{O-D} value averaged over the nuclear wave function, $\langle r_{O-D}\rangle$, is 1.078 Å, which compares with $\langle r_{O-D}\rangle$ = 1.109 Å for the given potential energy curve. This is typical of the H/D isotope effect observed in normal covalent bonds. For example, in gaseous H_2O and D_2O water molecules, the O−H and O−D bond lengths are 0.9724 and 0.9687 Å, respectively.[106] In fact, the shape of the potential energy curve in the region of $r_{O-H} < 1.3$ Å as shown in Figure 2a is very similar to a Morse potential for a regular O−H covalent bond. For covalent O−H bonds, $^{1}\Delta^{17}O(H/D)$ values are expected to be on the order of 1−2 ppm. For example, Wasylishen and Friedrich[107] reported $^{1}\Delta^{17}O(H/D)$ = 1.55 ppm in liquid water dissolved in cyclohexane-d_{12} at 20 °C. Raynes[108] reported an isotope shift of 4.04 ppm between gaseous $D_2{}^{17}O$ and $H_2{}^{17}O$ (approximately 2.02 ppm per D). Aime et al.[109] also reported some small $^{2}\Delta^{17}O(H/D)$ and $^{3}\Delta^{17}O(H/D)$ values (e.g., 0.13 ppm per D in DMSO).

The second model shown in Figure 2b can be characterized as an LBHB where the two energy minima are slightly different. In this case, the zero-point energy is comparable to the barrier height. The solved nuclear wave function for the ground state displays three important features. First, the nuclear wave function is now significantly delocalized as compared with that seen in Figure 2a. This feature is characteristic of an LBHB. Second, the nuclear wave function is centered at a longer OH distance with $\langle r_{O-H}\rangle$ = 1.289 Å. Third, the nuclear wave function shows an asymmetry between the two peaks, which is a consequence of the two asymmetric wells in the potential energy curve. More importantly, this asymmetry is greatly amplified on replacing H with D, resulting in a smaller $\langle r_{O-D}\rangle$ value, 1.243 Å. Thus, significant H/D isotope shifts are expected for the second model. The observed $^{1}\Delta^{17}O(H/D)$ isotope shifts for dibenzoylmethane seem to be consistent with this model. The nuclear wave functions from the third model, as shown in Figure 2c, are similar to those in Figure 2b, except that the asymmetry between the two peaks is absent. As a result, the values of $\langle r_{O-H}\rangle$ and $\langle r_{O-D}\rangle$ are practically the same, 1.319 versus 1.328 Å. Under this circumstance, no H/D isotope shifts are anticipated. The fact that we did not observe any significant $^{1}\Delta^{17}O(H/D)$ or $^{1h}\Delta^{17}O(H/D)$ isotope shifts in benzoylacetone and curcumin suggest that the potential energy curve described in the third model, Figure 2c, may be close to the situations in these two compounds. However, given the approximate nature of the three 1D models, all the above discussion should be considered to be qualitative.

To gain further information about the "location" of the enol hydrogen atom in these compounds, we applied a solid-state NMR technique known as 2D $^{17}O/^{1}H$ QD correlation spectroscopy[50] to directly measure the $^{1}H-^{17}O$ distances within the *cis*-keto−enol moiety. However, before we could apply this technique to the three 1,3-diketone compounds, it was important to examine on a model compound. To this end, we chose crystalline salicylic acid (2-hydroxybenzoic acid) with selectively ^{17}O-labeled oxygen atoms: [1,2-$^{17}O_2$]-salicylic acid and [3-^{17}O]-salicylic acid; see Figure 3. In these two samples, there are multiple $^{1}H-^{17}O$ distances that can be measured. As seen in Figure 3a, the salicylic acid molecules form hydrogen-bonded dimers in the solid state. In addition, the *ortho*-hydroxyl group in salicylic acid also forms an intramolecular O3−H2···O1═C hydrogen bond. Since double-proton transfer dynamics in salicylic acid dimers was proven to be extremely slow in our previous studies,[95,110] it was expected that the $^{1}H-^{17}O$ distance measurement in salicylic acid should produce reliable results. Figure 3 shows the 2D $^{17}O/^{1}H$ QD spectra for the two SA samples. For [1,2-$^{17}O_2$]-salicylic acid, two separate ^{17}O NMR signals are observed for O1 and O2 atoms. For the O2 signal, there is only one $^{1}H-^{17}O$ distance to measure, which is the O2−H1 bond length. As seen in Figure 3b, the projection of the O2 signal onto the indirect dimension produces a scaled dipolar powder pattern, which was analyzed by numerical simulations with SIMPSON.[99] For O2, we obtained a $^{1}H-^{17}O$ dipolar coupling constant of 15.2 ± 0.8 kHz, which corresponds to a $^{1}H-^{17}O$ distance of 1.02 ± 0.02 Å. Because we simulated only the splitting between the two "horns" in the F1 project of the 2D QD spectrum, such a splitting is insensitive to the relative orientation between the $^{1}H-^{17}O$ dipolar and ^{17}O EFG tensors.[50] Interestingly, the O1 atom in salicylic acid is at the center of two hydrogen bonds, O3−H2···O1···H1′−O2′, and thus is surrounded by the two nearest hydrogen atoms, H1′ and H2. As a result, the

https://doi.org/10.1021/acs.jpca.5c02392
J. Phys. Chem. A 2025, 129, 5993−6003

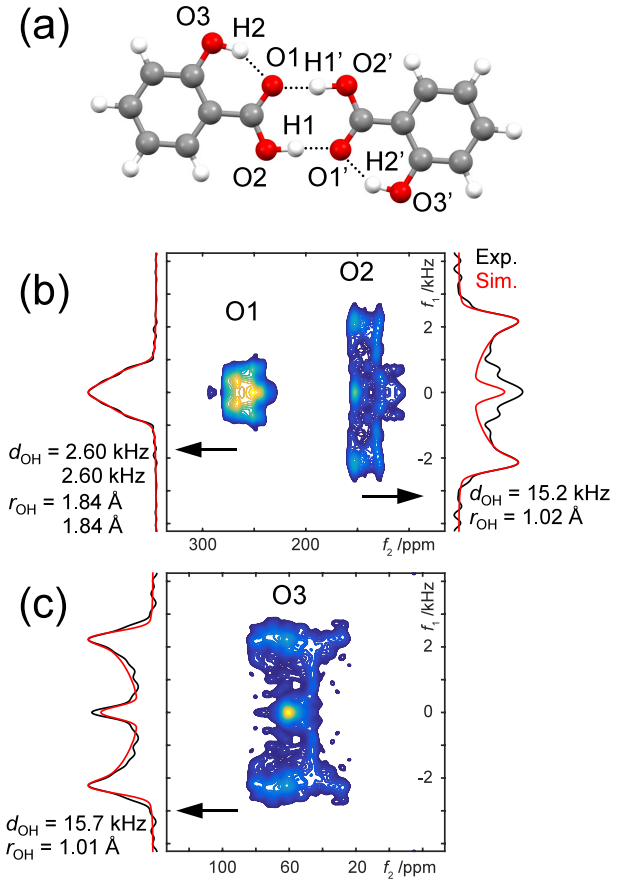

Figure 3. (a) Hydrogen bonding geometry in the dimeric structure of salicylic acid. 2D $^{17}O/^{1}H$ QD spectra of (b) [1,2-$^{17}O_2$]-salicylic acid and (c) [3-^{17}O]-salicylic acid. In (b) and (c), the experimental (black traces) and simulated (red traces) projections are shown where the $^{17}O-^{1}H$ dipolar couplings and the corresponding O−H distances used in the simulations are also listed. The true sample temperature in these experiments was 306 K.

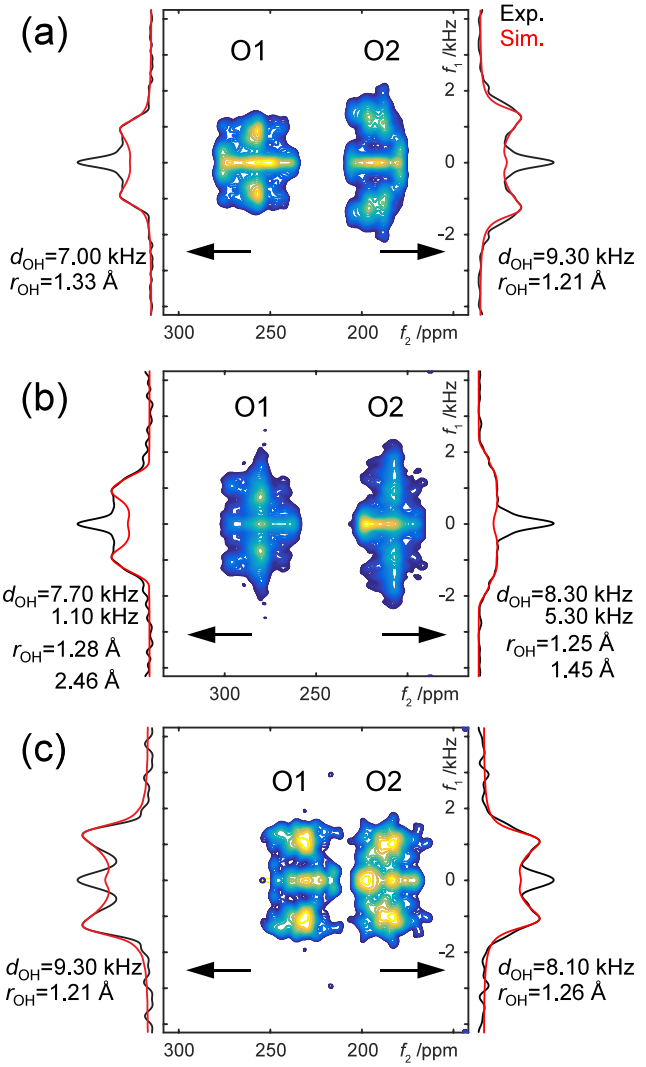

Figure 4. 2D $^{17}O/^{1}H$ QD spectra for (a) [1,2-$^{17}O_2$]-dibenzoylmethane, (b) [1,2-$^{17}O_2$]-benzoylacetone, and (c) [1,2-$^{17}O_2$]-curcumin. The experimental (black traces) and simulated (red traces) projections are shown where the $^{17}O-^{1}H$ dipolar couplings and the corresponding O−H distances used in the simulations are also listed. The true sample temperature in these experiments was 293 K.

projection of the O1 signal onto the indirect dimension displays a much smaller dipolar powder pattern with the "triplet" shape; see Figure 3b. Numerical simulations yielded two $^{1}H-^{17}O$ dipolar coupling constants of the same magnitude, 2.60 ± 0.8 kHz. This indicates that the two $^{1}H-^{17}O$ distances in the H2···O1···H1′ moiety are of the same length, 1.84 ± 0.02 Å. Figure 3c shows the 2D QD spectrum for [3-^{17}O]-salicylic acid, from which we determined the O3−H2 covalent bond length to be 1.01 ± 0.02 Å. We also performed the same 2D $^{17}O/^{1}H$ QD experiment for salicylic acid at a lower temperature (data not shown) and obtained spectra that are nearly identical to those in Figure 3. So, for the two salicylic acid samples, we measured a total of four $^{1}H-^{17}O$ distances (two O−H covalent bonds and two O···H hydrogen bonds). All the results are consistent with the crystal structure of salicylic acid and the optimized geometry. These results prove that the 2D QD methodology is valid for studying hydrogen-bonded systems.

Figure 4 displays the 2D $^{17}O/^{1}H$ QD results for dibenzoylmethane, benzoylacetone, and curcumin. In each case, two separate ^{17}O NMR signals are observed for O1 and O2. For dibenzoylmethane, we observed that the O1−H distance, 1.21 ± 0.02 Å, to be clearly shorter than the O2−H distance, 1.33 ± 0.02 Å. The case of benzoylacetone is slightly complicated because of the presence of short intramolecular contacts around both O1 and O2 atoms. The crystal structure of benzoylacetone indicates that, in addition to the enol hydrogen atom, O1 is in close contact with another hydrogen atom from a neighboring benzoylacetone molecule with an OH distance of 2.381 Å, while O2 is surrounded by three more hydrogen atoms with the OH distances of 2.391, 2.571, and 2.675 Å. As seen in Figure 4b, the F_1 projection of the O2 signal displays a "round-shaped" dipolar powder pattern (rather than having two sharp peaks), which is a clear indication of the multispin nature around the O2 atom. Since it is rather difficult to model a multispin system, we decided to simplify our numerical simulations by considering one short and one additional long $^{1}H-^{17}O$ distances for each of the O1 and O2 sites. We should note that it is the short $^{1}H-^{17}O$ distances that are related to the LBHB. For benzoylacetone, the two short OH distances were determined to be 1.28 ± 0.02 and 1.25 ± 0.02 Å for O1 and O2, respectively. This finding suggests that the enol hydrogen atom in benzoylacetone is close to the midpoint

https://doi.org/10.1021/acs.jpca.5c02392
J. Phys. Chem. A 2025, 129, 5993−6003

between the O1 and O2 atoms. An analysis of the 2D $^{17}O/^{1}H$ QD spectrum of curcumin yielded the two $^{1}H-^{17}O$ distances as 1.21 ± 0.02 and 1.26 ± 0.02 Å for O1 and O2, respectively; see Figure 4c. On the basis of the results shown in Figure 4, it is clear that the LBHB in dibenzoylmethane appears to be different from those in benzoylacetone and curcumin. That is, the LBHB in dibenzoylmethane exhibits a significant asymmetry whereas those in benzoylacetone and curcumin are more symmetric. This conclusion seems to be consistent with the trends observed in the H/D isotope shifts as discussed earlier.

It is instructive to link our new results on H/D isotope shifts and $^{1}H-^{17}O$ distances to both structural data and state-of-the-art MD simulation results available in the literature for the three 1,3-diketone compounds. Figure 5 summarizes the most

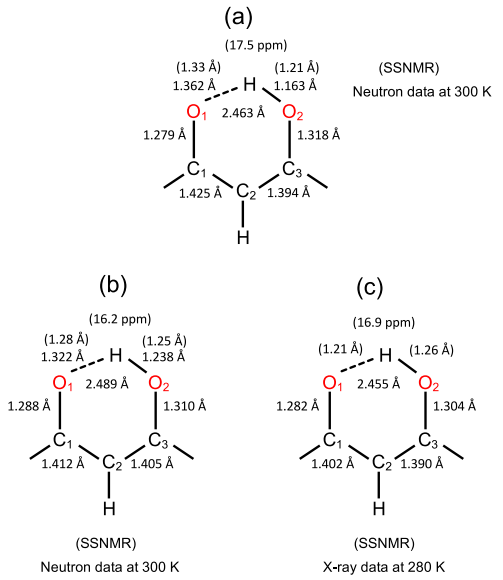

Figure 5. Selected bond lengths determined from high-quality neutron diffraction experiments for (a) dibenzoylmethane and (b) benzoylacetone and from X-ray diffraction experiments for (c) curcumin. The $^{1}H-^{17}O$ distances determined by SSNMR are shown in brackets. Also shown are the ^{1}H chemical shifts (in ppm) observed for the enol hydrogen atoms in these compounds.

accurate structural data found for the *cis*-keto−enol moieties of dibenzoylmethane, benzoylacetone, and curcumin. To make direct comparison, we chose crystal structures determined at temperatures close to those at which solid-state NMR data were collected. For dibenzoylmethane and benzoylacetone, single-crystal neutron diffraction data obtained at 300 K[61,62] are listed in Figure 5. For curcumin, however, all reported crystal structures were based on X-ray diffraction experiments, so the hydrogen positions are not as reliable as those determined by neutron diffraction studies. For this reason, we did not list the crystallographic OH distances for curcumin in Figure 5. For dibenzoylmethan, the neutron diffraction data suggest that the enol hydrogen is located asymmetrically between the two O atoms with the two OH distances being 1.163 and 1.362 Å. This asymmetry was also supported by a recent Hirshfeld atom refinement (HAR) analysis of the single-crystal X-ray diffraction data obtained at 100 K.[63] Our direct $^{1}H-^{17}O$ distance measurements, while being much less accurate than the neutron data, are nonetheless in agreement with the structural data. As discussed earlier, this asymmetry in the location of the enol hydrogen atom can explain the observed $^{1}\Delta^{17}O(H/D)$ or $^{1h}\Delta^{17}O(H/D)$ isotope shifts. All these observations support a potential energy curve as depicted in Figure 2b for dibenzoylmethane. In contrast, plane-wave DFT MD simulations performed by Kong et al.[32] seem to suggest that the two energy minima in dibenzoylmethane are quite symmetric. As seen in Figure 2b, a difference of 1−2 kJ/mol between the two energy minima can cause profound H/D effects. Because nuclear quantum effects are not treated explicitly in plane-wave DFT MD simulation, its accuracy is not expected to be sufficient to assess any energy difference of this small magnitude.

Benzoylacetone is another example with extensive crystallographic (X-ray and neutron diffraction) data available in the literature.[64−68] The accurate neutron structure obtained at 300 K suggests that the enol hydrogen atom in benzoylacetone is located very close to the midpoint between the two O atoms, with the two OH distances being 1.238 and 1.322 Å. Interestingly, Madsen et al.[68] found that, while the proton density in the residual Fourier map appears to be a broad flat distribution for the protonated benzoylacetone, the corresponding deuteron density map in the deuterated benzoylacetone exhibits two peaks. Their interpretation of this phenomenon was also based on a 1D potential energy curve that resembles the one shown in Figure 2c. Again, our observation of very small $^{1}\Delta^{17}O(H/D)$ or $^{1h}\Delta^{17}O(H/D)$ isotope shifts in benzoylacetone and the corresponding $^{1}H-^{17}O$ distance measurements are entirely consistent with the expectation from the potential shown in Figure 2c. For benzoylacetone, Durlak and Latajka[83] performed Car−Parrinello molecular dynamics (CPMD) and PIMD simulations for both the H- and D forms of the molecule. They found that, while the CPMD simulations predict a double-well potential energy surface with a very small asymmetry, the PIMD simulations, where nuclear quantum effects are treated explicitly, yielded a barrier-less potential surface. As a result, PIMD simulations suggest that the nuclear wave functions for the enol proton and deuteron are very similar in benzoylacetone. Our model shown in Figure 2c is thus consistent with the PIMD result.

For curcumin, although there are no accurate neutron diffraction data available in the literature, one may still be able to get clues about the nature of the LBHB from its high-quality X-ray crystal structure.[70] For example, the two C−O bonds within the *cis*-keto−enol moiety in curcumin are very similar, as seen in Figure 5, indicating that the enol hydrogen atom is probably close to the midpoint between the two O atoms. Indeed, our results on both the H/D isotope shifts and $^{1}H-^{17}O$ distances suggest that the LBHB in curcumin is more similar to benzoylacetone than to dibenzoylmethane.

Also listed in Figure 5 are the ^{1}H chemical shifts observed for the enol hydrogen atoms in these systems. As mentioned earlier, the observed ^{1}H chemical shifts of 17.5, 16.2, and 16.9 ppm are typical of those found in LBHBs. However, we should point out that, while the ^{1}H chemical shift has long been used as a spectroscopic handle to identify the presence of LBHBs, the three ^{1}H chemical shift values found in dibenzoylmethane, benzoylacetone, and curcumin do not seem to be a good predictor whether the enol hydrogen atom is located symmetrically or asymmetrically between the two O atoms. This aspect of LBHBs can be probed by H/D isotope shifts and direct $^{1}H-^{17}O$ distance measurement, as we have shown in this study.

https://doi.org/10.1021/acs.jpca.5c02392
J. Phys. Chem. A 2025, 129, 5993−6003

4. CONCLUSIONS

We have reported new solid-state ^{1}H, ^{13}C, and ^{17}O NMR data on three representative 1,3-diketone compounds: dibenzoylmethane, benzoylacetone, and curcumin. This is the first time that H/D isotope shifts on ^{13}C and ^{17}O nuclei are reported for LBHBs in the solid state. We showed that these H/D isotope shifts can be qualitatively rationalized on the basis of simplified 1D anharmonic potential energy curves for proton transfer across an LBHB. To accurately account for the H/D isotope shifts, detailed shapes of the ground-state nuclear wave functions must be known. In this study, we have also demonstrated that direct $^{1}H-^{17}O$ distance measurement with 2D $^{17}O/^{1}H$ QD correlation NMR spectroscopy offers another new way of probing the location of the enol hydrogen atom in 1,3-diketone molecules. The solid-state NMR results obtained for dibenzoylmethane and benzoylacetone are consistent with their high-quality neutron diffraction crystal structures in the literature. We have also obtained new insight into the LBHB in curcumin for which neutron diffraction data are unavailable. It has become clear to us that nuclear quantum effects are best probed with a combination of experimental (e.g., neutron/X-ray diffraction, solid-state NMR, IR, etc.) and theoretical (e.g., plane-wave DFT calculations and PIMD simulations) techniques. It is the complementary nature of these different techniques that may ultimately yield a unified description of LBHBs.

■ ASSOCIATED CONTENT

Supporting Information

The Supporting Information is available free of charge at https://pubs.acs.org/doi/10.1021/acs.jpca.5c02392.

Experimental and theoretical powder X-ray diffraction patterns for solid samples of dibenzoylmethane, benzoylacetone, and curcumin; experimental ^{13}C CP/MAS NMR spectra, experimental and simulated ^{17}O MAS NMR spectra for the H and D forms of dibenzoylmethane, benzoylacetone, and curcumin; detailed parameters for the 1D potential curves; sample input file for SIMPSON simulation (PDF)

■ AUTHOR INFORMATION

Corresponding Author

Gang Wu − *Department of Chemistry, Queen's University, Kingston, Ontario K7L 3N6, Canada;* orcid.org/0000-0002-0936-9432; Email: wugang@queensu.ca

Authors

Yizhe Dai − *Department of Chemistry, Queen's University, Kingston, Ontario K7L 3N6, Canada*

Ivan Hung − *Center of Interdisciplinary Magnetic Resonance, National High Magnetic Field Laboratory, Tallahassee, Florida 32310, United States;* orcid.org/0000-0001-8916-739X

Zhehong Gan − *Center of Interdisciplinary Magnetic Resonance, National High Magnetic Field Laboratory, Tallahassee, Florida 32310, United States;* orcid.org/0000-0002-9855-5113

Maria A. Matlinska − *Department of Chemistry, University of Alberta, Edmonton, Alberta T6G 2G2, Canada*

Roderick E. Wasylishen − *Department of Chemistry, University of Alberta, Edmonton, Alberta T6G 2G2, Canada*

Complete contact information is available at: https://pubs.acs.org/10.1021/acs.jpca.5c02392

Notes

The authors declare no competing financial interest.

■ ACKNOWLEDGMENTS

This work was supported by the Natural Sciences and Engineering Research Council (NSERC) of Canada through discovery grants to G.W. (RGPIN-2021-03140) and R.E.W. (RGPIN-2019-06816). We thank the Canada Foundation for Innovation (CFI) for a grant to purchase the 700 MHz NMR spectrometer at Queen's University. A portion of this work was performed at the National High Magnetic Field Laboratory (NHMFL), which is supported by the National Science Foundation Cooperative Agreement (DMR-2128556 and DMR-1644779) and the State of Florida. The NMR user facility at the NHMFL is also supported by NIH P41GM122698 and RM1GM148766. We are also grateful to Dr. Gabriele Schatte for assistance in recording powder X-ray diffraction patterns.

■ REFERENCES

(1) Benoit, M.; Marx, D.; Parrinello, M. Tunnelling and zero-point motion in high-pressure ice. *Nature* **1998**, *392* (6673), 258−261.

(2) Hammes-Schiffer, S. Hydrogen tunneling and protein motion in enzyme reactions. *Acc. Chem. Res.* **2006**, *39*, 93−100.

(3) Masgrau, L.; Roujeinikova, A.; Johannissen, L. O.; Hothi, P.; Basran, J.; Ranaghan, K. E.; Mulholland, A. J.; Sutcliffe, M. J.; Scrutton, N. S.; Leys, D. Atomic Description of an Enzyme Reaction Dominated by Proton Tunneling. *Science* **2006**, *312* (5771), 237−241.

(4) Klinman, J. P.; Kohen, A. Hydrogen tunneling links protein dynamics to enzyme catalysis. *Annu. Rev. Biochem.* **2013**, *82*, 471−496.

(5) Wang, L.; Isborn, C. M.; Markland, T. E. Simulating Nuclear and Electronic Quantum Effects in Enzymes. *Methods Enzymol.* **2016**, *577*, 389−418.

(6) Ceriotti, M.; Fang, W.; Kusalik, P. G.; McKenzie, R. H.; Michaelides, A.; Morales, M. A.; Markland, T. E. Nuclear Quantum Effects in Water and Aqueous Systems: Experiment, Theory, and Current Challenges. *Chem. Rev.* **2016**, *116*, 7529−7550.

(7) Markland, T. E.; Ceriotti, M. Nuclear quantum effects enter the mainstream. *Nat. Rev. Chem.* **2018**, *2*, No. 0109.

(8) Fang, W.; Chen, J.; Feng, Y.; Li, X.-Z.; Michaelides, A. The quantum nature of hydrogen. *Int. Rev. Phys. Chem.* **2019**, *38* (1), 35−61.

(9) Truhlar, D. G. Tunneling in enzymatic and nonenzymatic hydrogen transfer reactions. *J. Phys. Org. Chem.* **2010**, *23* (7), 660−676.

(10) Tuckerman, M. E.; Marx, D.; Klein, M. L.; Parrinello, M. On the quantum nature of the shared proton in hydrogen bonds. *Science* **1997**, *275* (5301), 817−820.

(11) Mei, H. S.; Tuckerman, M. E.; Sagnella, D. E.; Klein, M. L. Quantum Nuclear ab Initio Molecular Dynamics Study of Water Wires. *J. Phys. Chem. B* **1998**, *102* (50), 10446−10458.

(12) Schmitt, U. W.; Voth, G. A. The computer simulation of proton transport in water. *J. Chem. Phys.* **1999**, *111* (20), 9361−9381.

(13) Marx, D.; Tuckerman, M. E.; Hutter, J.; Parrinello, M. The nature of the hydrated excess proton in water. *Nature* **1999**, *397* (6720), 601−604.

(14) Billeter, S. R.; Webb, S. P.; Iordanov, T.; Agarwal, P. K.; Hammes-Schiffer, S. Hybrid approach for including electronic and nuclear quantum effects in molecular dynamics simulations of hydrogen transfer reactions in enzymes. *J. Chem. Phys.* **2001**, *114* (15), 6925−6936.

(15) Raugei, S.; Klein, M. L. Nuclear Quantum Effects and Hydrogen Bonding in Liquids. *J. Am. Chem. Soc.* **2003**, *125* (30), 8992−8993.
(16) Swalina, C.; Hammes-Schiffer, S. Impact of Nuclear Quantum Effects on the Molecular Structure of Bihalides and the Hydrogen Fluoride Dimer. *J. Phys. Chem. A* **2005**, *109* (45), 10410−10417.
(17) Swalina, C.; Wang, Q.; Chakraborty, A.; Hammes-Schiffer, S. Analysis of Nuclear Quantum Effects on Hydrogen Bonding. *J. Phys. Chem. A* **2007**, *111* (11), 2206−2212.
(18) Horsewill, A. J. Quantum tunnelling in the hydrogen bond. *Prog. Nucl. Magn. Reson. Spectrosc.* **2008**, *52* (2−3), 170−196.
(19) Li, X.-Z.; Walker, B.; Michaelides, A. Quantum nature of the hydrogen bond. *Proc. Natl. Acad. Sci. U. S. A.* **2011**, *108* (16), 6369−6373.
(20) Kanematsu, Y.; Tachikawa, M. Theoretical analysis of geometry and NMR isotope shift in hydrogen-bonding center of photoactive yellow protein by combination of multicomponent quantum mechanics and ONIOM scheme. *J. Chem. Phys.* **2014**, *141* (18), No. 185101.
(21) Wang, L.; Ceriotti, M.; Markland, T. E. Quantum fluctuations and isotope effects in *ab initio* descriptions of water. *J. Chem. Phys.* **2014**, *141* (10), No. 104502.
(22) Cleland, W. W. Low-barrier hydrogen bonds and low fractionation factor bases in enzymic reactions. *Biochemistry* **1992**, *31* (2), 317−319.
(23) Cleland, W. W.; Kreevoy, M. M. Low-barrier hydrogen bonds and enzymic catalysis. *Science* **1994**, *264* (5167), 1887−1890.
(24) Frey, P. A.; Whitt, S. A.; Tobin, J. B. A low-barrier hydrogen bond in the catalytic triad of serine proteases. *Science* **1994**, *264* (5167), 1927.
(25) Warshel, A.; Papazyan, A. Energy considerations show that low-barrier hydrogen bonds to not offer a catalytic advantage over ordinary hydrogen bonds. *Proc. Natl. Acad. Sci. U. S. A.* **1996**, *93* (24), 13665−13670.
(26) Cleland, W. W.; Frey, P. A.; Gerlt, J. A. The low barrier hydrogen bond in enzymic catalysis. *J. Biol. Chem.* **1998**, *273* (40), 25529−25532.
(27) Schutz, C. N.; Warshel, A. The low barrier hydrogen bond (LBHB) proposal revisited: the case of the Asp··· His pair in serine proteases. *Proteins* **2004**, *55*, 711−723.
(28) Thomas, L. H.; Florence, A. J.; Wilson, C. C. Hydrogen atom behaviour imaged in a short intramolecular hydrogen bond using the combined approach of X-ray and neutron diffraction. *New J. Chem.* **2009**, *33* (12), 2486−2490.
(29) Brunner, E.; Sternberg, U. Solid-state NMR investigations on the nature of hydrogen bonds. *Prog. Nucl. Magn. Reson. Spectrosc.* **1998**, *32* (1), 21−57.
(30) Aliev, A. E.; Harris, K. D. M. Probing hydrogen bonding in solids using solid state NMR spectroscopy. In *Supramolecular Assembly via Hydrogen Bonds I*; Structure and Bonding; Springer: 2004, *108*, 1−53, .
(31) Wu, G. Solid-state ^{17}O NMR studies of organic and biological molecules. *Prog. Nucl. Magn. Reson. Spectrosc.* **2008**, *52* (2−3), 118−169.
(32) Kong, X.; Brinkmann, A.; Terskikh, V.; Wasylishen, R. E.; Bernard, G. M.; Duan, Z.; Wu, Q.; Wu, G. Proton Probability Distribution in the O···H···O Low-Barrier Hydrogen Bond: A Combined Solid-State NMR and Quantum Chemical Computational Study of Dibenzoylmethane and Curcumin. *J. Phys. Chem. B* **2016**, *120* (45), 11692−11704.
(33) Lu, J.; Hung, I.; Brinkmann, A.; Gan, Z.; Kong, X.; Wu, G. Solid-state ^{17}O NMR reveals hydrogen-bonding energetics: Not all low-barrier hydrogen bonds are strong. *Angew. Chem., Int. Ed.* **2017**, *56*, 6166−6170.
(34) Marx, D.; Parrinello, M. Ab initio path-integral molecular dynamics. *Z. Phys. B: Condens. Matter* **1994**, *95* (2), 143−144.
(35) Marx, D.; Parrinello, M. Structural quantum effects and three-center two-electron bonding in CH_5^+. *Nature* **1995**, *375* (6528), 216−218.
(36) Marx, D.; Parrinello, M. Ab initio path integral molecular dynamics: basic ideas. *J. Chem. Phys.* **1996**, *104* (11), 4077−4082.
(37) Tuckerman, M. E.; Marx, D.; Klein, M. L.; Parrinello, M. Efficient and general algorithms for path integral Car-Parrinello molecular dynamics. *J. Chem. Phys.* **1996**, *104* (14), 5579−5588.
(38) Limbach, H. H.; Denisov, G. S.; Golubev, N. S. Hydrogen bond isotope effects studied by NMR. In *Isotope effects in chemistry and biology*, Kohen, A.; Limbach, H. H., Eds.; CRC Press: 2006; pp 193−280.
(39) McKenzie, R. H.; Bekker, C.; Athokpam, B.; Ramesh, S. G. Effect of quantum nuclear motion on hydrogen bonding. *J. Chem. Phys.* **2014**, *140* (17), No. 174508.
(40) Hansen, P. E. Isotope effects on chemical shifts in the study of intramolecular hydrogen bonds. *Molecules* **2015**, *20*, 2405−2424.
(41) Dračínský, M. The chemical bond: The perspective of NMR spectroscopy. *Annu. Rep. NMR Spectrosc.* **2017**, *90*, 1−40.
(42) Altman, L. J.; Laungani, D.; Gunnarsson, G.; Wennerstrom, H.; Forsen, S. Proton, deuterium, and tritium nuclear magnetic resonance of intramolecular hydrogen bonds. Isotope effects and the shape of the potential energy function. *J. Am. Chem. Soc.* **1978**, *100*, 8264−8266.
(43) Reuben, J. Intramolecular hydrogen bonding as reflected in the deuterium isotope effects on carbon-13 chemical shifts. Correlation with hydrogen bond energies. *J. Am. Chem. Soc.* **1986**, *108* (8), 1735−1738.
(44) Hansen, P. E. Deuterium isotope effects on the ^{13}C nuclear shielding of intramolecularly hydrogen-bonded systems. *Magn. Reson. Chem.* **1986**, *24*, 903−910.
(45) Hansen, P. E.; Ibsen, S. N.; Kristensen, T.; Bolvig, S. Deuterium and ^{18}O isotope effects on ^{13}C chemical shifts of sterically hindered and/or intramolecularly hydrogen-bonded o-hydroxy acyl aromantics. *Magn. Reson. Chem.* **1994**, *32*, 399−408.
(46) Bolvig, S.; Hansen, P. E. Deuterium-induced isotope effects on ^{13}C chemical shifts as a probe for tautomerism in enolic beta-diketones. *Magn. Reson. Chem.* **1996**, *34*, 467−478.
(47) Bolvig, S.; Hansen, P. E.; Morimoto, H.; Wemmer, D.; Williams, P. Primary tritium and deuterium isotope effects on chemical shifts of compounds having an intramolecular hydrogen bond. *Magn. Reson. Chem.* **2000**, *38*, 525−535.
(48) Liepins, E.; Petrova, M. V.; Gudriniece, E.; Paulins, J.; Kuznetsov, S. L. Relationships between ^{1}H, ^{13}C and ^{17}O NMR chemical shifts and H/D isotope effects on ^{13}C and ^{17}O nuclear shielding in intramolecular hydrogen-bonded systems. *Magn. Reson. Chem.* **1989**, *27*, 907−915.
(49) Bolvig, S.; Hansen, P. E.; Wemmer, D.; Williams, P. Deuterium isotope effects on ^{17}O chemical shifts of intramolecularly hydrogen bonded systems. *J. Mol. Struct.* **1999**, *509*, 171−181.
(50) van Beek, J. D.; Dupree, R.; Levitt, M. H. Symmetry-based recoupling of ^{17}O−^{1}H spin pairs in magic-angle spinning NMR. *J. Magn. Reson.* **2006**, *179*, 38−48.
(51) Wu, G. Solid-State ^{17}O NMR studies of organic and biological molecules: Recent advances and future directions. *Solid State Nucl. Magn. Reson.* **2016**, *73*, 1−14.
(52) Wu, G. ^{17}O NMR studies of organic and biological molecules in aqueous solution and in the solid state. *Prog. Nucl. Magn. Reson. Spectrosc.* **2019**, *114−115*, 135−191.
(53) van Eck, E. R. H.; Smith, M. E. Orientation of the quadrupole and dipole tensors oh hydroxyl groups by ^{17}O quadrupole separated local field NMR. *J. Chem. Phys.* **1998**, *108*, 5904−5912.
(54) Brinkmann, A.; Kentgens, A. P. M. Proton-selective ^{17}O−^{1}H distance measurements in fast magic-angle-spinning solid-state NMR spectroscopy for the determination of hydrogen bond lengths. *J. Am. Chem. Soc.* **2006**, *128*, 14758−14759.
(55) Brinkmann, A.; Kentgens, A. P. M. Sensitivity Enhancement and Heteronuclear Distance Measurements in Biological ^{17}O Solid-State NMR. *J. Phys. Chem. B* **2006**, *110* (32), 16089−16101.
(56) Goswami, M.; Madhu, P. K. Combining dipolar-quadrupolar correlation spectroscopy with isotropic shift resolution in magic-angle-spinning ^{17}O NMR. *J. Magn. Reson.* **2012**, *219*, 4−12.

https://doi.org/10.1021/acs.jpca.5c02392
J. Phys. Chem. A 2025, 129, 5993−6003

(57) Carnahan, S. L.; Lampkin, B. J.; Naik, P.; Hanrahan, M. P.; Slowing, I. I.; VanVeller, B.; Wu, G.; Rossini, A. J. Probing O-H Bonding through Proton Detected ^{1}H−^{17}O Double Resonance Solid-State NMR Spectroscopy. *J. Am. Chem. Soc.* **2019**, *141* (1), 441−450.
(58) Hoelger, C.-G.; Limbach, H.-H. Localization of Hydrons in Hydrogen Bonds Using Dipolar Solid State NMR Spectroscopy. *J. Phys. Chem.* **1994**, *98* (45), 11803−11810.
(59) Yaghmaei, S.; Khodagholian, S.; Kaiser, J. M.; Tham, F. S.; Mueller, L. J.; Morton, T. H. Chelation of a Proton by an Aliphatic Tertiary Diamine. *J. Am. Chem. Soc.* **2008**, *130* (25), 7836−7838.
(60) Williams, D. E. Crystal structure of dibenzoylmethane. *Acta Crystallogr.* **1966**, *21* (3), 340−349.
(61) Jones, R. D. G. The crystal structure of the enol tautomer of 1,3-diphenyl-1,3-propanedione (dibenzoylmethane) by neutron diffraction. *Acta Crystallogr. Sect. B* **1976**, *32* (6), 1807−1811.
(62) Jones, R. D. G. The crystal and molecular structure of the enol form of 1-phenyl-1,3-butanedione (benzoylacetone) by neutron diffraction. *Acta Crystallogr. Sect. B* **1976**, *32* (7), 2133−2136.
(63) Wojtulewski, S.; Strawa, J. W.; Tomczyk, M.; Gawel, M.; Brzezinski, K. A new look at two polymorphic crystal structures of dibenzoylmethane: relationship between the crystal packing and the hydrogen atom position revealed by quantum chemistry and quantum crystallography methods. *Acta Crystallogr. Sect. B* **2020**, *76* (6), 957−966.
(64) Semmingsen, D.; Larsson, L. O.; Nyberg, B.; Huhtikangas, A.; Pearson, W. B.; Meisalo, V. The crystal structure of benzoylacetone. *Acta Chem. Scand.* **1972**, *26*, 143−154.
(65) Winter, W.; Zeller, K.-P.; Berger, S. On the structure of the enol benzoylacetone. *Z. Naturforsch. B* **1979**, *34*, 1606−1611.
(66) Madsen, G. K. H.; Iversen, B. B.; Larsen, F. K.; Kapon, M.; Reisner, G. M.; Herbstein, F. H. Topological Analysis of the Charge Density in Short Intramolecular O−H···O Hydrogen Bonds. Very Low Temperature X-ray and Neutron Diffraction Study of Benzoylacetone. *J. Am. Chem. Soc.* **1998**, *120* (39), 10040−10045.
(67) Herbstein, F. H.; Iversen, B. B.; Kapon, M.; Larsen, F. K.; Madsen, G. K. H.; Reisner, G. M. X-ray and neutron diffraction study of benzoylacetone in the temperature range 8−300 K: comparison with other cis-enol molecules. *Acta Crystallogr. B* **1999**, *55*, 767−787.
(68) Madsen, G. K. H.; McIntyre, G. J.; Schiøtt, B.; Larsen, F. K. The low-barrier hydrogen bond of deuterated benzoylacetone probed by very low temperature neutron and X-ray diffraction studies and theoretical calculations. *Chem. - Eur. J.* **2007**, *13*, 5539−5547.
(69) Tønnesen, H. H.; Karlsen, J.; Mostad, A.; Samuelsson, B.; Enzell, C. R.; Berg, J. E. Structural studies of curcuminoids. I. The crystal structure of curcumin. *Acta Chem. Scand.* **1982**, *36*, 475−479.
(70) Parimita, S. P.; Ramshankar, Y. V.; Suresh, S.; Guru Row, T. N. Redetermination of curcumin: (1E,4Z,6E)-5-hydroxy-1,7-bis(4-hydroxy-3-methoxyphenyl)hepta-1,4,6-trien-3-one. *Acta Crystallogr., Sect. E* **2007**, *63* (2), o860−o862.
(71) Sanphui, P.; Goud, N. R.; Khandavilli, U. B. R.; Bhanoth, S.; Nangia, A. New polymorphs of curcumin. *Chem. Commun.* **2011**, *47* (17), 5013−5015.
(72) Etter, M. C.; Reutzel, S. M.; Vojta, G. M. Analysis of isotropic chemical shift data from high-resolution solid-state NMR studies of hydrogen-bonded organic compounds. *J. Mol. Struct.* **1990**, *237*, 165−185.
(73) Vila, A. J.; Lagier, C. M.; Olivieri, A. C. Carbon-13 NMR and AM1 study of the intramolecular proton transfer in solid 1,3-diphenylpropane-1,3-dione. *J. Chem. Soc., Perkin Trans. 2* **1990**, No. 9, 1615−1618.
(74) Vila, A. J.; Lagier, C. M.; Olivieri, A. C. Proton transfer in solid 1-phenylbutane-1,3-dione and related 1,3-diones as studied by ^{13}C CPMAS NMR spectroscopy and AM1 calculations. *J. Phys. Chem.* **1991**, *95*, 5069−5073.
(75) Emmler, T.; Gieschler, S.; Limbach, H. H.; Buntkowsky, G. A simple method for the characterization of OHO-hydrogen bonds by ^{1}H-solid state NMR spectroscopy. *J. Mol. Struct.* **2004**, *700* (1−3), 29−38.
(76) Kong, X.; Terskikh, V.; Toubaei, A.; Wu, G. A solid-state ^{17}O NMR study of platinum-carboxylate complexes: carboplatin and oxaliplatin. *Can. J. Chem.* **2015**, *93* (9), 945−953.
(77) Matlinska, M.; Wasylishen, R. E.; Bernard, G. M.; Terskikh, V. V.; Brinkmann, A.; Michaelis, V. K. Capturing elusive polymorphs of Curcumin: A structural characterization and computational study. *Cryst. Growth Des.* **2018**, *18*, 5556−5563.
(78) Poeppler, A.-C.; Luebtow, M. M.; Schlauersbach, J.; Wiest, J.; Meinel, L.; Luxenhofer, R. Loading-Dependent Structural Model of Polymeric Micelles Encapsulating Curcumin by Solid-State NMR Spectroscopy. *Angew. Chem., Int. Ed.* **2019**, *58* (51), 18540−18546.
(79) Dai, Y.; Terskikh, V.; Brinmkmann, A.; Wu, G. Solid-state ^{1}H, ^{13}C, and ^{17}O NMR characterization of the two uncommon polymorphs of curcumin. *Cryst. Growth Des.* **2020**, *20*, 7484−7491.
(80) Schiøtt, B.; Iversen, B. B.; Hellerup Madsen, G. K.; Bruice, T. C. Characterization of the Short Strong Hydrogen Bond in Benzoylacetone by ab Initio Calculations and Accurate Diffraction Experiments. Implications for the Electronic Nature of Low-Barrier Hydrogen Bonds in Enzymatic Reactions. *J. Am. Chem. Soc.* **1998**, *120* (46), 12117−12124.
(81) Gilli, P.; Bertolasi, V.; Pretto, L.; Ferretti, V.; Gilli, G. Covalent versus Electrostatic Nature of the Strong Hydrogen Bond: Discrimination among Single, Double, and Asymmetric Single-Well Hydrogen Bonds by Variable-Temperature X-ray Crystallographic Methods in β-Diketone Enol RAHB Systems. *J. Am. Chem. Soc.* **2004**, *126* (12), 3845−3855.
(82) Milovanovic, B.; Stankovic, I. M.; Petkovic, M.; Etinski, M. Elucidating Solvent Effects on Strong Intramolecular Hydrogen Bond: DFT-MD Study of Dibenzoylmethane in Methanol Solution. *ChemPhysChem* **2019**, *20* (21), 2852−2859.
(83) Durlak, P.; Latajka, Z. Car-Parrinello and path integral molecular dynamics study of the intramolecular hydrogen bonds in the crystals of benzoylacetone and dideuterobenzoylacetone. *Phys. Chem. Chem. Phys.* **2014**, *16* (42), 23026−23037.
(84) Etinski, M.; Ensing, B. Puzzle of the Intramolecular Hydrogen Bond of Dibenzoylmethane Resolved by Molecular Dynamics Simulations. *J. Phys. Chem. A* **2018**, *122* (28), 5945−5954.
(85) Etter, M. C.; Jahn, D. A.; Urbanczyk-Lipkowska, Z. A new polymorph of dibenzoylmethane. *Acta Crystallogr. Sect. D* **1987**, *43* (2), 260−263.
(86) Kaitner, B.; Mestrovic, E. Structure of a new crystal modification of 1,3-diphenyl-1,3-propanedione. *Acta Crystallogr. Sect. D* **1993**, *49* (8), 1523−1525.
(87) Thorat, A. A.; Dalvi, S. V. Solid-State Phase Transformations and Storage Stability of Curcumin Polymorphs. *Cryst. Growth Des.* **2015**, *15* (4), 1757−1770.
(88) Dong, S.; Ida, R.; Wu, G. A combined experimental and theoretical O-17 NMR study of crystalline urea: An example of large hydrogen-bonding effects. *J. Phys. Chem. A* **2000**, *104* (47), 11194−11202.
(89) Yamada, K.; Dong, S.; Wu, G. Solid-state O-17 NMR investigation of the carbonyl oxygen electric-field-gradient tensor and chemical shielding tensor in amides. *J. Am. Chem. Soc.* **2000**, *122* (47), 11602−11609.
(90) Wu, G.; Dong, S.; Ida, R.; Reen, N. A solid-state ^{17}O nuclear magnetic resonance study of nucleic acid bases. *J. Am. Chem. Soc.* **2002**, *124* (8), 1768−1777.
(91) Kwan, I. C. M.; Mo, X.; Wu, G. Probing Hydrogen Bonding and Ion-Carbonyl Interactions by Solid-State ^{17}O NMR Spectroscopy: G-Ribbon and G-Quartet. *J. Am. Chem. Soc.* **2007**, *129* (8), 2398−2407.
(92) Tang, A. W.; Kong, X.; Terskikh, V.; Wu, G. Solid-State ^{17}O NMR of Unstable Acyl-Enzyme Intermediates: A Direct Probe of Hydrogen Bonding Interactions in the Oxyanion Hole of Serine Proteases. *J. Phys. Chem. B* **2016**, *120* (43), 11142−11150.
(93) Dai, Y.; Wu, G. Solid-state ^{17}O NMR studies of sulfonate jump dynamics in crystalline sulfonic acids: Insights into the hydrogen bonding effect. *J. Phys. Chem. A* **2020**, *124*, 9597−9604.

https://doi.org/10.1021/acs.jpca.5c02392
J. Phys. Chem. A 2025, 129, 5993−6003

(94) Wu, G.; Dai, Y.; Hung, I.; Gan, Z.; Terskikh, V. $^{1}H/^{17}O$ Chemical Shift Waves in Carboxyl-Bridged Hydrogen Bond Networks in Organic Solids. *J. Phys. Chem. A* **2024**, *128* (21), 4288−4296.
(95) Kong, X.; Shan, M.; Terskikh, V.; Hung, I.; Gan, Z.; Wu, G. Solid-State ^{17}O NMR of Pharmaceutical Compounds: Salicylic Acid and Aspirin. *J. Phys. Chem. B* **2013**, *117* (33), 9643−9654.
(96) Thurber, K. R.; Tycko, R. Measurement of sample temperatures under magic-angle spinning from the chemical shift and spin-lattice relaxation rate of ^{79}Br in KBr powder. *J. Magn. Reson.* **2009**, *196*, 84−87.
(97) Taylor, R. E. ^{13}C CP/MAS: Application to glycine. *Concepts Magn. Reson., Part A* **2004**, *22A* (2), 79−89.
(98) Harris, R. K.; Becker, E. D.; Cabral de Menezes, S. M.; Goodfellow, R.; Granger, P. NMR Nomenclature: Nuclear Spin Properties and Conventions for Chemical Shifts: IUPAC Recommendations 2001. *Solid State Nucl. Magn. Reson.* **2002**, *22* (4), 458−483.
(99) Bak, M.; Rasmussen, J. T.; Nielsen, N. C. SIMPSON: A General Simulation Program for Solid-State NMR Spectroscopy. *J. Magn. Reson.* **2000**, *147* (2), 296−330.
(100) Bolvig, S.; Hansen, P. E. Isotope effects on chemical shifts as an analytical tool in structural studies of intramolecular hydrogen bonded compounds. *Curr. Org. Chem.* **2000**, *4*, 19−54.
(101) Jameson, C. J. The isotope shift in NMR. *J. Chem. Phys.* **1977**, *66*, 4983−4988.
(102) Grzesiek, S.; Cordier, F.; Dingley, A. J. Scalar couplings across hydrogen bonds. *Methods Enzymol.* **2001**, *338*, 111−133.
(103) Levine, I. N. Numerical solution of the one-dimensional time-independent Schrodinger equation. In *Quantum Chemistry*, 7th ed.; Pearson: 2014.
(104) Jameson, C. J. The dynamic and electronic factors in isotope effects on NMR parameters. In *Isotopes in the Physical and Biomedical Science*; Burncel, E.; Jameson, C. J., Eds.; Elsevier Science Publishers B. V.: 1991; Vol. 2; pp 1−54.
(105) Jameson, C. J. Isotope Effects on Chemical Shifts and Coupling Constants. In *eMagRes.*; Harris, R. K.; Wasylishen, R. E., Eds.; Wiley: 2007.
(106) Cook, R. L.; De Lucia, F. C.; Helminger, P. Molecular force field and structure of water: Recent microwave results. *J. Mol. Spectrosc.* **1974**, *53* (1), 62−76.
(107) Wasylishen, R. E.; Friedrich, J. O. Deuterium isotope effects on nuclear magnetic shielding constants and spin-spin coupling constants in the ammonium ion, ammonia, and water. *Can. J. Chem.* **1987**, *65*, 2238−2243.
(108) Raynes, W. T. The oxygen-17 nuclear magnetic shielding in water-^{17}O and water-d_2-^{17}O. *Mol. Phys.* **1983**, *49* (2), 443−447.
(109) Aime, S.; Santucci, E.; Fruttero, R. Deuterium isotope effects on oxygen-17 chemical shifts. *Magn. Reson. Chem.* **1986**, *24* (10), 919−920.
(110) Wu, G.; Hung, I.; Gan, Z.; Terskikh, V.; Kong, X. Solid-State ^{17}O NMR Study of Carboxylic Acid Dimers: Simultaneously Accessing Spectral Properties of Low- and High-Energy Tautomers. *J. Phys. Chem. A* **2019**, *123* (38), 8243−8253.

https://doi.org/10.1021/acs.jpca.5c02392
J. Phys. Chem. A 2025, 129, 5993−6003